Point defects in ordered metallic compounds. II. Self-consistent studies of vacancies in FeAl

J. M. Koch, N. Stefanou, and C. Koenig
Laboratoire de Magnétisme et de Structure Electronique des Solides, Université Louis Pasteur—4, rue Blaise Pascal, 67070 Strasbourg Cedex, France
(Received 21 October 1985)

Ab initio self-consistent electronic-structure calculations of vacancies in ordered stoichiometric FeAl within the linear-muffin-tin-orbital atomic-sphere-approximation method are presented. The potential and local densities of states on the defect and the charge perturbations on its neighboring sites in the matrix are calculated and discussed in relation with numerous experimental results concerning the effect of small departures from stoichiometry for this ordered compound.

I. INTRODUCTION

Many experimental studies on ordered metallic binary compounds in a CsCl structure have been performed during the last 15 years especially on FeAl, CoAl, NiAl, and CoGa.[1-7] Near the stoichiometry, several types of defects exist in these compounds. In particular, vacancies on both sublattices and antistructural defects responsible for the appearance of magnetism were found. We shall especially consider here the case of FeAl. At low temperature, it has been shown that for iron concentrations higher than 0.5, the Fe atoms in excess occupy antisite positions on the Al sublattice and form magnetic clusters with their neighbors.[8,9] Different experimental values of the local moment have been proposed, the interpretation of the measurements being a quite difficult problem.[10] For an excess of aluminum, a quite different behavior is observed. The Al atoms occupy Al sites whereas vacancies appear on the Fe sublattice. Vacancy concentration increases with increasing Al content up to 52% Al. Contrary to the cases of NiAl and CoAl, antistructural Al defects are present too and at 52% Al the $FeAl_2$ phase appears.[11,12] In the equiatomic compound, the vacancy concentration remains quite high even at low temperature. This is thought to be due to the difficulty of formation (and then elimination) of vacancy clusters in strongly ordered FeAl. Vacancy elimination occurs preferentially in localized regions by interaction with dislocations.[13-16] At low temperature, the most probable vacancy is the vacancy on the iron sublattice with eight Al nearest neighbors. At high temperature, the increase of disorder leads to an evolution of the vacancy distribution towards an equipartition on both sublattices.[11,12] We are interested in the theoretical study of vacancies in this compound as it is the first step towards the understanding of its off-stoichiometric states. The work presented here is one of the first *ab initio* self-consistent calculations of the electronic structure of localized defects in ordered compounds taking correctly into account the crystalline structure of the host. The linear-muffin-tin—orbital (LMTO) formalism applied to substitutional defects is described in great detail in the preceding paper (I) (Ref. 17, denoted as KSK hereafter) and the same notation is used in this paper.

The band structures of the "pure" host crystals are calculated using the standard LMTO procedure including the so-called "combined corrections" beyond the atomic-sphere approximation (ASA).[18] The electronic structure of the hosts as well as the defect potentials are obtained self-consistently within the density functional theory, exchange and correlation effects being included in the local-density approximation.[19] The electronic structure of defects is calculated within the single-site approximation, i.e., the perturbing potential is supposed to be localized in the central sphere and the modifications induced in the potentials on the neighbors are neglected. The ASA is not corrected in the impurity (or vacancy) sphere but we show in Sec. II with a few examples that this difference of treatments leads to very small errors. In the same section we also discuss some practical aspects of the numerical calculation and give a brief description of a single vacancy in pure Al and pure Fe. The most important part of this paper is the study of single vacancies on each of the two sublattices in FeAl, developed in Sec. III. The conclusions drawn from these calculations are given in the last section.

II. NUMERICAL ASPECTS—ACCURACY

A. Complex contour integration

The determination of the spatial electronic charge density $\rho(\mathbf{r})$, which is an essential physical quantity in the density functional theory requires an integration of the Green function over the energies up to the Fermi level E_F:

$$\rho(\mathbf{r}) = -\frac{1}{\pi} \operatorname{Im} \int_{-\infty}^{E_F} G(\mathbf{r},\mathbf{r};E)dE \ . \tag{2.1}$$

The core states are treated apart and kept frozen in the atomic potentials during the whole self-consistent procedure. To perform the integration (2.1) for the valence states on the real axis with a sufficient accuracy, approximately 1000 points from the bottom of the band to E_F are needed. As shown in detail in KSK, the extension of the Green function to a complex argument z allows to replace this integral by an integral along a contour in the upper complex plane performed on a much smaller number of

TABLE I. Total numbers of electrons in Fe and Al sites in FeAl and charge perturbation δq^1 induced by a single vacancy on one first neighbor in the host, calculated by integration along a complex path with different numbers of z points.

Number of z points	N_{Fe}	N_{Al}	Vacancy at Fe site $10\times\delta q^1$	Vacancy at Al site $10\times\delta q^1$
97	8.294	2.7064	−0.9238	−1.916
49	8.309	2.7063	−0.9238	−1.908
25	8.394	2.7059	−0.9236	−1.884

points. The valence part of the charge density is then [KSK, Eq. (6.8)]:

$$\rho_v(\mathbf{r})=-\frac{1}{\pi}\mathrm{Im}\oint_{Z_{\mathrm{inf}}}^{E_F} G(\mathbf{r},\mathbf{r};z)dz \ . \tag{2.2}$$

The chosen contour is of rectangular shape, starting below the bottom of the valence band but above the upper core states energy (i.e., $Z_{\mathrm{inf}}=E_F-1$ Ry for Al, Fe, and FeAl), running at 0.3 Ry above the real axis and ending at E_F.

As a numerical test, we have calculated the number of electrons N^{Fe} and N^{Al} in the Fe and Al spheres in ordered FeAl, using a complex contour integration with 97, 49, and 25 z points (Table I). They can be compared to their "true" values in the ordered compound calculated within the standard LMTO method and given in Table II. The same test was done for the charge perturbation δq^1 induced on one first neighbor by a vacancy at a Fe and an Al site in FeAl (see Sec. III). N^{Al} and δq^1 are very stable and 50 z points are sufficient to get a good agreement between the two methods. When high densities of states with sharp structures are present around the Fermi level, more z points are necessary to perform an accurate integration and special care must be taken when approaching E_F (along the third segment of the contour). This is the case for the Fe site where it is obvious that N^{Fe} is less stable with respect to the number of z points. For that reason, we usually take 97 points along the path with a finer grid along the third segment, i.e., with, respectively, 13, 49, . . . , and 37 equally spaced points along the three segments, corresponding to energy intervals of 0.025, 0.021, and 0.008 Ry (the test given in Table I corresponds to one-half or one-fourth of these points).

To control the convergence, the mean square difference between the input and output potentials,

$$D=\left[\frac{3}{4\pi S^3}\int_0^S r^2 dr[V_{\mathrm{in}}(r)-V_{\mathrm{out}}(r)]^2\right]^{1/2}, \tag{2.3}$$

is calculated at each iteration. Typically, for paramagnetic impurities, the iterative procedure is performed until D becomes less than 10^{-5}.

B. Atomic-sphere approximation

As we have already mentioned, all of our calculations are performed within the atomic-sphere approximation which means that the radius S of the muffin-tin potential spheres is taken to be equal to the Wigner-Seitz radius. In ordered structures, the Hamiltonian matrix elements are renormalized to correct the bad overlap of these spheres.[18] In the dilute alloy, an impurity is substituted to an atom of the compound in the same sphere with the same radius, all relaxation effects being neglected; for the self-consistent procedure in the defect sphere, the "combined corrections" are not included (KSK).

The simplest way to get an idea of the errors caused by this difference of treatment is to consider a pure metal or an ordered compound and treat one of its atoms as a substitutional impurity at the same place. We did this test for four different fictitious alloys: we considered an Al "impurity" in pure aluminum, a Fe and an Al "impurity" on their own sublattices in FeAl, and a Fe impurity in ferromagnetic iron. In Table III, we compare the partial and total numbers of electrons in the "host" and "impurity" spheres. In the nonmagnetic cases, Al and FeAl, the errors are negligible. Five to ten iterations on the impurity site give modifications of less than 10^{-4} electrons in Al and 10^{-3} electrons in FeAl. Ferromagnetic iron is the most sensitive case: we find a departure of 0.018 electrons in the total number of electrons and 0.036 Bohr magnetons in the total moment. Three remarks must be made.

(i) In the band-structure calculation of the hosts, the integrations in the Brillouin zone (BZ) are performed with a grid of 946 **k** points in the $\frac{1}{48}$th of the BZ for fcc structures (aluminum), 969 for CsCl structures (FeAl), and 506

TABLE II. Partial and total numbers of electrons in the Fe and Al sites in "pure" ordered FeAl and partial and total numbers of electrons in the defect sphere for a single vacancy on the Fe and the Al sublattice, respectively.

	Ordered compound		Dilute alloy	
	Fe site	Al site	Vacancy at Fe site	Vacancy at Al site
N_s	0.602	0.914	0.416	0.377
N_p	0.785	1.373	0.473	0.418
N_d	6.907	0.419	0.126	0.152
N_{tot}	8.294	2.706	1.015	0.947

TABLE III. Partial and total number of electrons and local magnetic moment (M) for Al, FeAl, and Fe calculated (1) within the standard LMTO method and (2) as a fictitious impurity (see the text).

	Al		Al site in FeAl		Fe site in FeAl		Ferromagnetic Fe			
	(1)	(2)	(1)	(2)	(1)	(2)	↓(1)↑		↓(2)↑	
N_s	1.1257	1.1257	0.9135	0.9139	0.6022	0.6045	0.328	0.317	0.328	0.316
N_p	1.4531	1.4530	1.3733	1.3741	0.7848	0.7889	0.425	0.372	0.427	0.374
N_d	0.4212	0.4212	0.4194	0.4195	6.9068	6.9001	2.140	4.418	2.165	4.408
N_{tot}	3.0000	2.9999	2.7062	2.7075	8.2938	8.2935	8.000		8.018	
M	0	0	0	0	0	0	2.414		2.178	
D		$\leq 10^{-5}$		$\leq 10^{-5}$		$\leq 10^{-5}$			$\leq 10^{-3}$	

for bcc structures (iron). More accuracy may be achieved for Fe by using a finer **k** points grid.

(ii) Besides, it is well known that the combined corrections have a more important effect for open structures like the bcc (or CsCl) crystals than for closed-packed fcc structures. Hence, the difference in the treatment of the host and impurity atoms is more pronounced in Fe or FeAl compared to Al. Nevertheless, the results in FeAl are quite good even for the Fe d states.

(iii) For a nonmagnetic defect, the Madelung term in the self-consistent potential has to be determined at each iteration as an additional constant V_M to satisfy Friedel's screening rule (KSK). This constant converges and becomes stable after five to ten iterations. In ferromagnetic defects, the total displaced charge is the sum of the two different displaced charges $\Delta Z^{\uparrow}(E_F)$ and $\Delta Z^{\downarrow}(E_F)$. It is obvious that the determination of two constants $V_{M\uparrow}$ and $V_{M\downarrow}$ insuring together that

$$\Delta Z^{\uparrow}(E_F)+\Delta Z^{\downarrow}(E_F)=Z-\bar{Z}^{0} \tag{2.4}$$

[KSK Eq. (5.2)] is a more unstable procedure. This is certainly the main origin to the larger inaccuracy observed in ferromagnetic iron. During the self-consistent procedure, $V_{M\uparrow}$ and $V_{M\downarrow}$ converge indeed towards a unique couple of stable values but the convergence is slower than in the paramagnetic case.

C. Vacancies in pure aluminum and iron

Before presenting the study of vacancies in the ordered binary compound FeAl, we give briefly some results concerning single vacancies in pure aluminum and pure ferromagnetic iron. It will be interesting to compare the numbers of electrons in the vacancy spheres to those in FeAl. We obtain 0.532 electrons in the Wigner-Seitz sphere for the vacancy in Al and 0.541 electrons for a vacancy in Fe. The corresponding results are given in Table IV where the two spins in the case of a Fe host have not been separated because the local magnetic moment calculated on the vacancy is negligibly small. They are consistent with previous studies of vacancies in Al, treated in the jellium[20] or the pseudopotential[21] approximations although a detailed comparison is difficult since the total charge in the vacancy Wigner-Seitz sphere is not clearly indicated in these latter works. They are also of the same order of magnitude as those recently obtained by the Green-function method[22,23] for vacancies in copper, yielding a charge of 0.67 electrons in the vacancy sphere in the single-site approximation and 1.1 electrons for a cluster calculation. We recall, as discussed in KSK, that in these KKR calculations, Friedel's screening rule is only insured in the cluster scheme, whereas it is always satisfied in our calculations.

III. VACANCIES IN FeAl

A. Stoichiometric ordered FeAl

The electronic band structure of ordered FeAl in CsCl structure calculated within the LMTO method has already been published.[24] The present results differ slightly from the previous ones mainly because of the inclusion of the combined corrections and the scalar relativistic effects.

The partial and total densities of states (DOS) on Fe and Al are shown in Fig. 1. They present the general characteristics of transition-metal aluminides (TAl).

(i) Two d peaks separated by a deep minimum in the transition-metal density.

(ii) A strong hybridization between the Al p states and the T d states and a repulsion effect between the Al s states and the T d states pointed out by a very low s density in regions of high Fe d peaks.

TABLE IV. Partial and total numbers of electrons in pure Al and Fe, and for a single vacancy in Al and Fe.

			Pure Fe		
	Pure Al	Vacancy in pure Al	↑	↓	Vacancy in pure Fe
N_s	1.126	0.163	0.328	0.317	0.228
N_p	1.453	0.249	0.425	0.372	0.214
N_d	0.421	0.120	2.140	4.418	0.099
N_{tot}	3.000	0.532	2.893	5.107	0.541

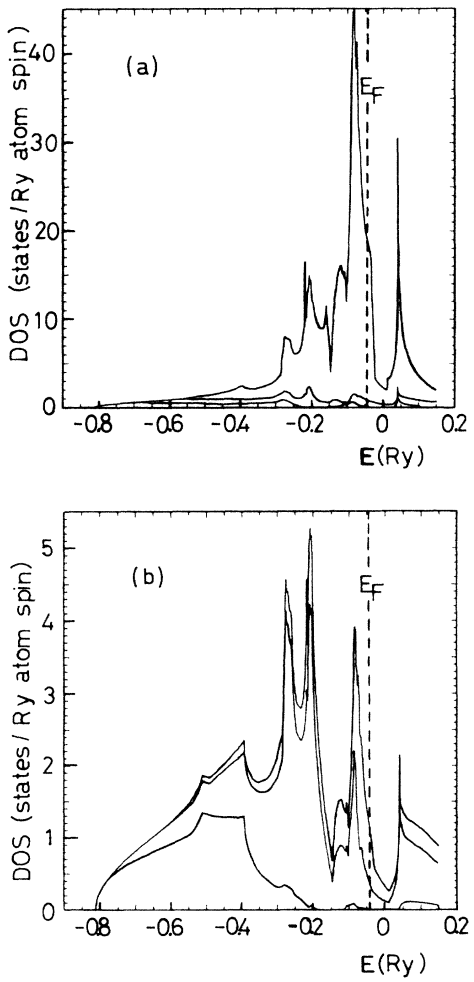

FIG. 1. Partial DOS in ordered FeAl ($s, s+p, s+p+d$): (a) on a Fe site and (b) on an Al site.

(iii) An electron transfer from the Al site to the transition-metal site, this transfer being equal to 0.294 electrons in the case of FeAl (Table II).

The position of the Fermi level, whether it is situated in one of the two d peaks or in the minimum, will have important consequences on the physical properties of the considered TAl compound. In FeAl, E_F lies in the upper verge of the first d peak and the density of states at E_F is therefore quite high: $n(E_F)=41.0$ states Ry^{-1} FeAl^{-1} compared to $n(E_F)=40.1$ states Ry^{-1} FeAl^{-1} in Ref. 24. The electronic specific-heat coefficient may be evaluated from $n(E_F)$ by

$$\gamma=\frac{\pi^2 k_B^2}{3} n(E_F) \tag{3.1}$$

when the electron-phonon interaction is neglected (k_B is the Boltzman constant). We find $\gamma=7.1$ mJ mole^{-1} K^{-2}, which is higher than the only estimation available from experiment: $\gamma=5.5$ mJ mole^{-1} K^{-2}.[25] It seems to be clear now that this discrepancy between theory and experience for FeAl is due to magnetic effects.[9] The samples used for the measurements did not show a pure paramagnetic behavior; the experimental value of the specific-heat coefficient was separated into a pure electronic contribution γ and a magnetic contribution γ_m. No precise determination of γ_m has been performed. In FeAl, even at exact stoichiometry and low temperature, few magnetic clusters are present. This is confirmed by the position of E_F in the first d resonance which indicates that the paramagnetic situation must be quite unstable.

B. Single vacancies in FeAl

We have considered both types of vacancies existing in FeAl: a vacancy at a Fe site and a vacancy at an Al site.

1. *Vacancy charge—Friedel's screening rule*

The partial and total numbers of electrons in the defect sphere are shown in Table II. The vacancy is essentially screened by electrons with locally "s" and "p" symmetry and the total vacancy charges, 1.015 and 0.947 electrons, respectively, for Fe and Al sites, are again quite high, even higher than what was found in pure iron and aluminum (Sec. II C).

In our calculations, the vacancy potential satisfies Friedel's screening rule (2.4), and we wish to emphasize here the essential part played by this rule in the determination of the defect charge. We recall [KSK Eq. (5.6)] that, in the paramagnetic case, the total displaced charge up to the energy E is given by

$$\Delta Z(E)=\Delta N_c+\frac{2}{\pi}\sum_L \Lambda_L(E)\ , \tag{3.2}$$

ΔN_c being the difference between the numbers of core electrons in the defect and the host atoms (for a vacancy, $\Delta N_c=-\bar{N}_c$ on the considered host site). The generalized phase shift $\Lambda_L(E)$ is defined as

$$\Lambda_L(E)=-\mathrm{Im}\ln\left[\frac{\bar{P}_l^0(E)}{P_l^0(E)}\{\Sigma_{LL}(E)[P_l^0(E)-\bar{P}_l^0(E)]+1\}\right]+\pi\Delta N_L^*(E)\ , \tag{3.3}$$

where ΔN_L^* is the difference per spin of the additional bound states appearing below E at energies E_l^* in the LMTO potentials for the defect and the host atoms. In (3.3), $P_l^0(E)$ and $\bar{P}_l^0(E)$ are monotonic increasing functions of the energy, depending only upon the potential of the defect and the host atom, respectively.[18] The matrix elements $\Sigma_{LL}(E)$ are directly related to the densities of states $\bar{n}_L^0(E)$ on the central site in the host and their Hilbert transforms [KSK, Eq. (4.10)].[26–28] Equation (3.3) shows that the value of the total displaced charge up to the Fermi level [$\Delta Z(E_F)$] results from the combined effects of the relative heights of the defect and host potentials and the characteristics of the band structure of the host crystal at the Fermi level.

$P_l^0(E_F)$ and $\Delta N_L^*(E_F)$ are the only quantities in (3.3) depending upon the nature of the defect. For a vacancy, $P_l^0(E_F)$ is the only one which varies during the self-consistent procedure. Actually, $P_l^0(E_F)$ is much more

sensitive to the height of the potential than to the details of its shape. To illustrate this point, we have represented in Fig. 2 the self-consistent vacancy potentials for both types of vacancies in FeAl and compare them to the repulsive square barrier potentials which subtract the same charge from the conduction band: eight electrons for a vacancy at a Fe site and three electrons for a vacancy at an Al site. In the case of the square barrier, the vacancy contains 1.07 electrons and 1.00 electrons, respectively, at a Fe site and an Al site. Obviously, this simple square barrier model already gives a good estimation of the vacancy charge, provided that Friedel's screening rule is satisfied.

A second point which has to be distinguished is the strong dependence of the vacancy charge upon the band structure of the host, i.e., upon the values of $\bar{P}_l^0$ and Σ_{LL} at E_F. For example, in the pure metals Al and Fe, we obtain roughly half the charge found for the corresponding vacancies in FeAl. To understand this fact, we consider again a square barrier to describe the vacancy. Figure 3 compares the evolution of the total displaced charge $\Delta Z(E_F)-\Delta N_c$ versus the height of the square barrier for a vacancy in pure Fe and at a Fe site in FeAl [Fig. 3(a)] as well as for a vacancy in pure Al and at an Al site in FeAl [Fig. 3(b)]. This evolution is approximately linear but the positions and the slopes of the straight lines are quite different in the compound compared to the pure metals, which is essentially an effect of the differences in the electronic structures of the hosts. It is clear that a more repulsive barrier is necessary in pure Al and Fe to repel the same charge as in FeAl. Therefore, the local charges in the vacancy spheres are smaller. On the other hand, the rather steep slope of the four curves illustrates the sensitivity of the total displaced charge $\Delta N(E_F)$ (hence also the local charge) to the height of the barrier.

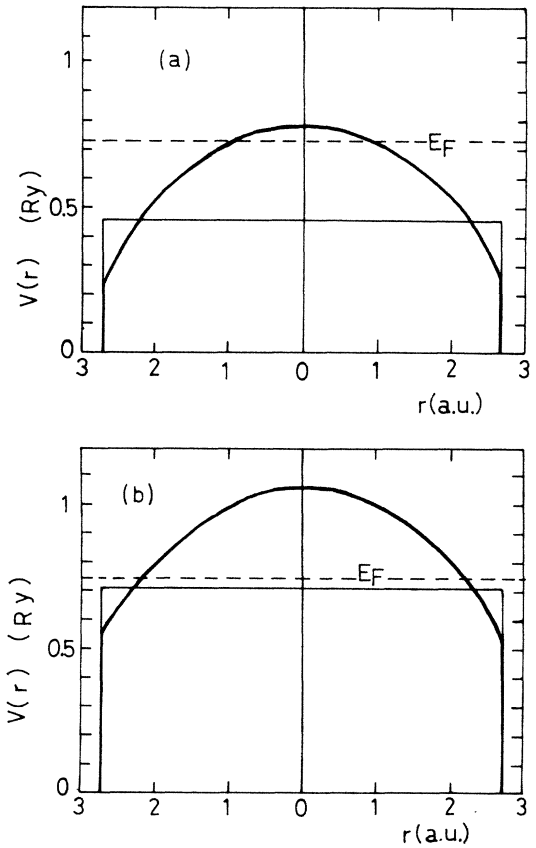

FIG. 2. Vacancy potentials in FeAl. The bold solid line is the self-consistent potential on the vacancy and the solid line is the square barrier necessary to repell the same charge. The origin of potentials is taken at the muffin-tin value (V_{MTZ}). Common Wigner-Seitz radius: $S=2.706$ a.u. (a) Vacancy at Fe site. (b) Vacancy at Al site.

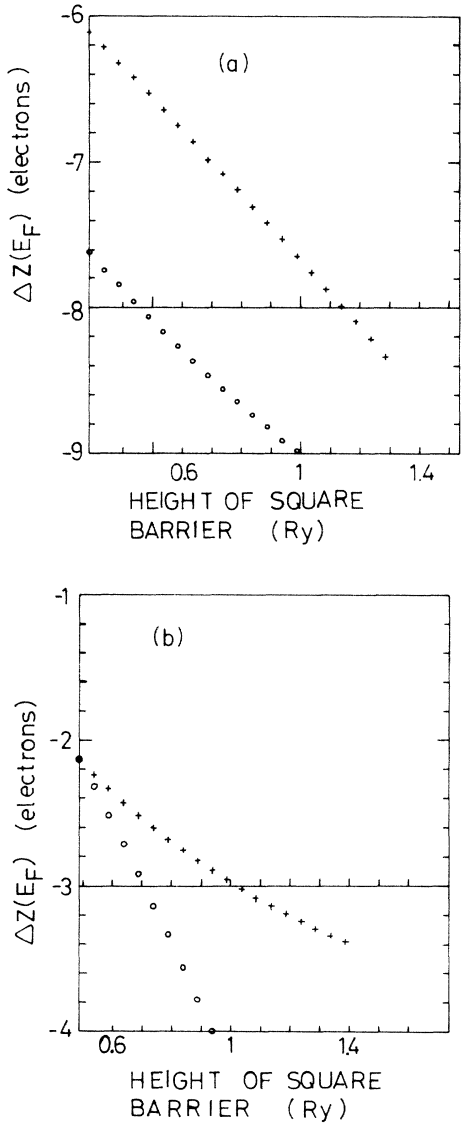

FIG. 3. Variation of the total displaced charge $\Delta Z(E_F)-\Delta N_c$ with respect to the potential height for a square barrier: (a) Simple vacancy in Fe (+) and at a Fe site in FeAl (○). Friedel's screening rule is satisfied for $\Delta Z(E_F)-\Delta N_c=-8$. (b) Single vacancy in Al (+) and at an Al site in FeAl (○). Friedel's screening rule is satisfied for $\Delta Z(E_F)-\Delta N_c=-3$.

2. *Density of states—phase shifts*

In order to get a more detailed understanding of the electronic structure of the vacancy, the partial densities of states on the defect site (Fig. 4) and the corresponding phase shifts (Fig. 5) have been represented for the s, p, and d symmetries. For each type of vacancy, three DOS curves are given: the "s" density, the sum of the "s" and "p" densities $[\sum_{L=1}^{4} n_L(E)]$ and the total "$s+p+d$" density $[\sum_{L=1}^{9} n_L(E)]$. The generalized phase shifts $\Lambda_L(E)$ have been gathered into the four irreducible representations of the group O_h: s,p (threefold degenerated), $d_{25'}$ and d_{12} (respectively, threefold and twofold degenerated), $\Lambda_\Gamma(E)=\sum_{L\in\Gamma}\Lambda_L(E)$. The vacancy potential being more repulsive than the host potentials, these phase shifts are negative. In the local DOS, two different types of behavior can be clearly distinguished.

(i) In energy regions where the potential functions $P_l^0(E)$ and $\bar{P}_l^0(E)$ calculated in the defect and host spheres, respectively, are close to each other, the partial density of states on the vacancy $n_L^0(E)$ follows the variation of the corresponding density on the substituted host

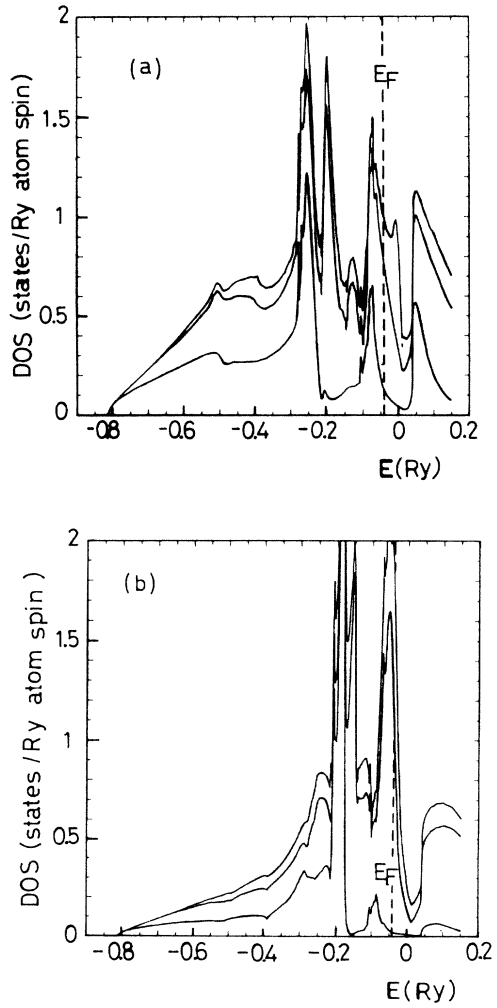

FIG. 4. Local DOS on the vacancy ($s, s+p, s+p+d$). (a) Vacancy at Fe site. (b) Vacancy at Al site.

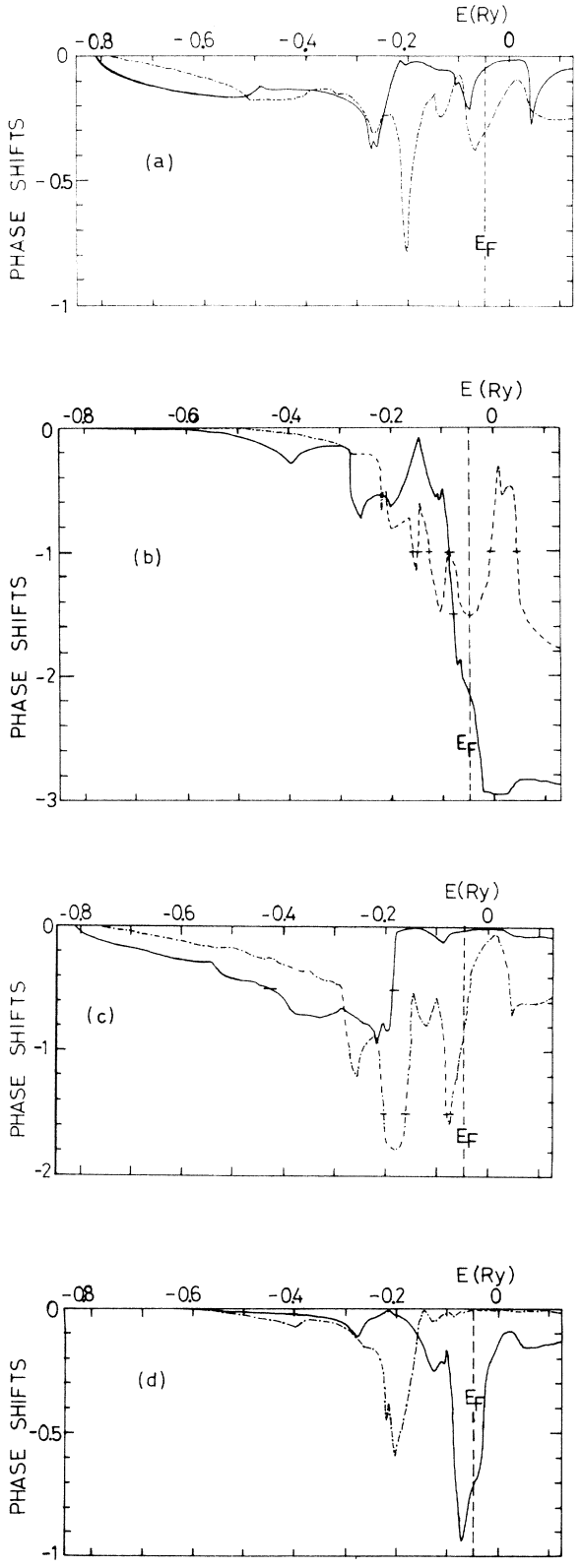

FIG. 5. Generalized phase shifts (x degeneracy $/\pi$). The little horizontal strokes indicate the energies $\tilde{E}_L$ solutions of the resonance condition (3.4). (a) Vacancy at Fe site: s (solid line) and p (dashed line). (b) Vacancy at Fe site: $d_{25'}$ (solid line) and d_{12} (dashed line). (c) Vacancy at Al site: s (solid line) and p (dashed line). (d) Vacancy at Al site: $d_{25'}$ (solid line) and d_{12} (dashed line).

atom $\bar{n}_L^0(E)$. This is transparent in the equation relating the defect DOS $n_L^0(E)$ to the host DOS $\bar{n}_L^0(E)$:

$$n_L^0(E)=\frac{(\dot{P}_l/\dot{\bar{P}}_l)\bar{n}_L(E)}{[1+\mathrm{Re}\Sigma_{LL}(P_l^0-\bar{P}_l^0)]^2+[\mathrm{Im}\Sigma_{LL}(P_l^0-\bar{P}_l^0)]^2} . \tag{3.4}$$

For instance, the partial "s" and "p" local DOS on the vacancy at a Fe site in FeAl [Fig. 4(a)] reproduce the structures existing in the "s" and "p" DOS on the Fe sites in "pure" FeAl [Fig. 1(a)]; this is also the case for the d states on the vacancy at an Al site. This type of behavior corresponds to low values of the phase shifts.

(ii) Some of the peaks in the local DOS on the defect are due to resonances, occurring in regions of low host densities of states $\bar{n}_L^0(E)$ at energies $\tilde{E}_L$ satisfying the resonance condition [KSK, Eq. (4.11)]

$$1+\mathrm{Re}\Sigma_{LL}(P_l^0-\bar{P}_l^0)=0 . \tag{3.5}$$

This situation corresponds to higher absolute values of the phase shifts and at each energy $\tilde{E}_L$ solution of (3.5), $\Lambda_L(\tilde{E}_L)$ is equal to $-\pi/2$. In Fig. 5, these energies are indicated with a horizontal mark. Notice that a resonance will occur only if $\bar{n}_L^0(\tilde{E}_L)$ is sufficiently low, as can be easily deduced from (3.4). For the vacancy at an Al site, two solutions to (3.5) were found for the s symmetry and four solutions for the p symmetry; sharp resonances are observed in the local s states at $\tilde{E}_s=-0.18$ Ry and in the local p states at $\tilde{E}_p=-0.16$ Ry and $\tilde{E}_p=-0.07$ Ry. No resonance occurs in the d states since they are less important and close to the host d states.

For the vacancy at an Fe site, the situation is inverted: the local "s" and "p" states are close to those of the host Fe atom whereas one solution $\tilde{E}_L$ for the $d_{25'}$ representation and 7 solutions for d_{12} were found. The most visible resonances in these "d" states correspond to the solutions $\tilde{E}_{d_{25'}}=-0.08$ Ry and $\tilde{E}_{d_{12}}=-0.005$ Ry.

Once more, the band structure of the host plays a considerable role in the behavior of the vacancy. For instance, the hybridization of the Al s states with the Fe d states in ordered FeAl gives rise to a drastic decrease in the Al s density in regions of important Fe d peaks, allowing possible resonances in the local vacancy s states at these energies. On the contrary in pure Al, the s density is much more regular and no resonance occurs in the vacancy DOS; this observation is coherent with the fact that the vacancy charge in pure Al is lower. The resonant behavior of the vacancy DOS in the compound can be interpreted as an enhancement of the penetration of electrons into the vacancy by tunneling effect. A comparable resonant behavior was obtained by Klima *et al.*[29] for a single vacancy in TiN. A last remark can be made on the local DOS concerning the stability of vacancies in the compound FeAl: For the vacancy on the Al sublattice, the total density of states has greater peaks placed at higher energies than for the vacancy on the Fe sublattice; this indicates that the vacancy has probably a higher total energy when situated on the Al sublattice. This is in agreement with the fact that the vacancy seems to be less stable at an Al site than at a Fe site, although all the energy contributions to the physical situation have not been taken into account.

From the change in the total number of states due to the vacancy, the change $\Delta\gamma$ in the electronic specific-heat coefficient can be estimated:

$$\Delta\gamma=\frac{C\pi^2k_B^2}{3}\left|\frac{d}{dE}\Delta Z(E)\right|_{E_F} , \tag{3.6}$$

where C is the vacancy concentration per molecule of FeAl. We find $\Delta\gamma=-1.2\times C$ mJ mole^{-1} K^{-2} and $\Delta\gamma=15.1\times C$ mJ mole^{-1} K^{-2}, respectively, for vacancies on the Fe sublattice and the Al sublattice. In the most probable case at low temperature, vacancies at Fe sites, the tendency is to lower the electronic specific-heat coefficient, but it must be noticed that in both cases, the values of $\Delta\gamma$ are very small.

3. *Charge perturbation on the neighbors*

The charge perturbation δq^τ induced by the vacancy in each neighboring sphere in the host is given by the integration along the complex contour of the difference between the imaginary parts of the defect and host Green functions in the sphere τ:

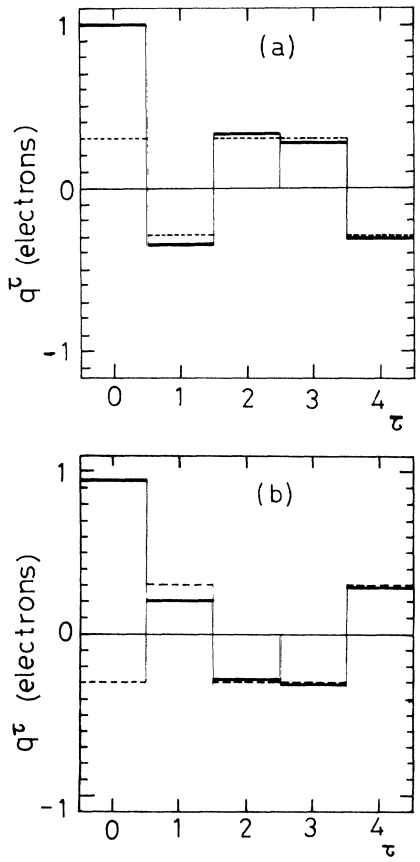

FIG. 6. Departure from neutrality in each sphere around the vacancy site, for atoms belonging to the first four neighboring shells (solid lines), compared to the situation in ordered FeAl (dashed lines). (a) Vacancy at Fe site. (b) Vacancy at Al site.

TABLE V. Charge perturbation induced by the vacancy in the central site ($\delta q^{(0)}$) and the first four neighboring shells ($\delta q^{(n)}, n=1,4$). N_n is the number of neighbors in shell n and $\sum_n \delta q^{(n)}$ is the sum of the charge perturbation up to the nth shell.

Shell	N_n	Vacancy at Fe site $\delta q^{(n)}$	Vacancy at Fe site $\sum_n \delta q^{(n)}$	Vacancy at Al site $\delta q^{(n)}$	Vacancy at Al site $\sum_n \delta q^{(n)}$
$n=0$	1	0.721	0.721	1.241	1.241
$n=1$	8	−0.739	−0.018	−1.530	−0.289
$n=2$	6	0.404	0.386	0.073	−0.216
$n=3$	12	−0.514	−0.128	−0.078	−0.294
$n=4$	24	−0.074	−0.202	−0.104	−0.398

$$\delta q^{\tau} = -\frac{1}{\pi} \int_S d^3r \,\mathrm{Im} \int_{Z_{\inf}}^{E_F} dz [G(\mathbf{r},\mathbf{r};z) - \bar{G}(\mathbf{r},\mathbf{r};z)] \,. \quad (3.7)$$

It must be noticed that δq^{τ} is not computed by a numerical difference of G and $\bar{G}$, since the LMTO theory developed in KSK provides the analytical expression of this difference [KSK, Eq. (6.9)]. Therefore the values of δq^{τ}, although they are quite small as can be seen in Fig. 6, are still significant. On the other hand, the small values of δq^{τ} justify the single-site approximation, neglecting the modifications in the neighboring potentials. The charge perturbation in the whole nth shell is then

$$\delta q^{(n)} = \sum_{\tau \in n} \delta q^{\tau} \,. \quad (3.8)$$

The values of $\delta q^{(n)}$ ($n=1,4$) are given in Table V. Of course, it must be noticed that the values of $\delta q^{(4)}$ on the 24 atoms of the fourth shell is only qualitative, the numerical uncertainty being of the order of magnitude of the value δq^{τ} on each atom. By adding the charge perturbations $\delta q^{(n)}$ to the value $\delta q^{(0)}$ of the total charge variation in the defect sphere with respect to the host crystal, we get an idea of the extension of the perturbation, since the total sum must be equal to zero. The results given in Table V show clearly that a vacancy at a Fe site is more rapidly screened than a vacancy at an Al site. In the first case, the charge perturbation induced by the vacancy in the central site is nearly cancelled by the variation in its first neighboring shell, and only 2.5% of the total screening charge (−8 electrons) are missing in the first four shells. For a vacancy at an Al site, the perturbation is more extended and 0.4 electrons are missing in the first four shells which represents 13.3% of the total screening charge (−3 electrons).

This conclusion is confirmed when looking at the departure from neutrality $q^{\tau} = \bar{q}^{\tau} + \delta q^{\tau}$ in each sphere around the vacancy (Fig. 6). In the ordered stoichiometric compound, the charge transfer from Al to Fe leaves an extra number of electrons $\bar{q}^{\mathrm{Fe}} = 0.294$ electrons on the Fe sites and $\bar{q}^{\mathrm{Al}} = -0.294$ electrons on the Al sites. When a vacancy is created on the Fe sublattice, the departure from neutrality in the central sphere q^0, which is equal to the vacancy charge, has the same sign and is increased with respect to the corresponding value $\bar{q}^{\mathrm{Fe}}$ in the host. This enhancement is compensated by an opposite variation of q^1 on the first Al neighbors. In this case, the charge perturbation due to the vacancy follows the tendency induced in the host by the respective electronegativities of the two constituents and even reinforces it. On the contrary, when the vacancy is created on the Al sublattice, the sign of the central charge is reversed and, consequently, the positive q^1 on the first Fe neighbors is lowered. This is opposed to the natural charge transfer in the compound and hence represents a much more important perturbation to the FeAl crystal. It explains clearly why the Al vacancies are more extended defects and less likely to appear in this compound. This result confirms what was observed in the local density of states and is in complete agreement with the experimental data.[11,12]

IV. CONCLUSION

The LMTO-ASA method is well-suited to the studies of ordered compounds and dilute alloys with several atoms per unit cell. With the technique of complex integration, the Green function has to be determined for only 100 or even less complex arguments. Energy-dependent quantities such as the local density of states and the phase shifts are calculated once when self-consistency is achieved.

As a first step in the study of small departure from stoichiometry in *T*Al compounds, we examined the case of vacancies in FeAl and showed that the vacancy at an Al site, which is less stable than the vacancy at a Fe site, is a more important perturbation to the ordered FeAl crystal. The vacancy charge is quite high in both cases and its sensitivity to the electronic structure of the host has been discussed. Our results show clearly that a vacancy cannot be described by an infinite square barrier.

A quite different behavior can be expected for vacancies in other TAl compounds, since the position of the Fermi level with respect to the low-density region between the two d peaks varies from one case to the other. A more detailed study of TAl and other CsCl compounds including Al antistructural defects will be published in the near future. Calculation of interaction energy of point defects is also under progress.

ACKNOWLEDGMENTS

The numerical work was done on a CRAY-1 computer (Palaiseau) under a Centre National de la Recherche Scientifique Research Project.

[1]E. Wachtel, V. Linse, and V. Gerold, J. Phys. Chem. Solids **34**, 1461 (1973).
[2]J. J. Begot, R. Caudron, P. Faivre, and P. Costa, J. Phys. Lett. **35**, L125 (1974).
[3]A. Amamou and F. Gautier, J. Phys. F **4**, 563 (1974).
[4]J. G. Booth and R. G. Pritchard, J. Phys. F **5**, 347 (1975).
[5]R. Cywinski and J. G. Booth, J. Phys. F **6**, L75 (1975).
[6]K. Endo, I. An, and A. Shinogi, J. Phys. F **7**, 199 (1977).
[7]E. H. Waterman and J. J. M. Franse, J. Phys. F **10**, 947 (1980).
[8]G. R. Caskey, J. M. Franz, and D. J. Sellmyer, J. Phys. Chem. Solids **34**, 1179 (1973).
[9]R. Kuentzler, J. Phys. **44**, 1167 (1983).
[10]H. Domke and L. K. Thomas, J. Magn. Magn. Mater. **45**, 305 (1984).
[11]D. Paris, Thèse d'Etat, Université, Pierre et Marie Curie, Paris VI, 1979 (unpublished).
[12]D. Paris and P. Lesbats, J. Nucl. Mater. **69-70**, 628 (1978).
[13]T. Eguchi, Y. Tomokiyo, and C. Kinoshita, J. Phys. Paris Colloq. **12**, C7-382 (1977).
[14]D. Weber, M. Meurtin, D. Paris, A. Fourdeux, and P. Lesbats, J. Phys. Paris Colloq. **12**, C7-332 (1977).
[15]A. Fourdeux and P. Lesbats, Philos. Mag. A **45**, 81 (1982).
[16]D. Paris and P. Lesbats, J. Phys. Paris Colloq. **12**, C7-364 (1977).
[17]C. Koenig, N. Stefanou, and J. M. Koch, Phys. Rev. B **33**, 5307 (1986).
[18]O. K. Andersen, Phys. Rev. B **12**, 3060 (1975).
[19]L. Hedin and B. I. Lundqvist, J. Phys. C **4**, 2064 (1971).
[20]M. Manninen and R. M. Nieminen, J. Phys. F **8**, 2243 (1978).
[21]B. Chakraborty, R. W. Siegel, and W. E. Pickett, Phys. Rev. B **24**, 5445 (1981).
[22]R. Zeller and P. J. Braspenning, Solid State Commun. **42**, 701 (1982).
[23]P. J. Braspenning, R. Zeller, A. Lodder, and P. H. Dedrichs, Phys. Rev. B **29**, 703 (1984).
[24]C. Koenig and M. A. Khan, Phys. Rev. B **27**, 6129 (1983).
[25]H. Okamoto and P. A. Beck, Monatsh. Chem. **103**, 907 (1972).
[26]C. Koenig and E. Daniel, J. Phys. **42**, L193 (1981).
[27]C. Koenig, P. Léonard, and E. Daniel, J. Phys. **42**, 1015 (1981).
[28]P. Léonard and N. Stefanou, Philos. Mag. B **51**, 151 (1985).
[29]J. Klima, G. Schadler, P. Weinberger, and A. Neckel, J. Phys. F **15**, 1307 (1985).